REPORT DOCUMENTATION PAGE

Form Approved
OMB No. 0704-0188

1. REPORT DATE *(DD-MM-YYYY)*	2. REPORT TYPE	3. DATES COVERED *(From - To)*
02-08-2011	Journal Article	

4. TITLE AND SUBTITLE
Holographic Interferometry of Oil Films and Droplets in Water with a Single-beam Mirror-type Scheme

5a. CONTRACT NUMBER

5b. GRANT NUMBER

5c. PROGRAM ELEMENT NUMBER
N/A

6. AUTHOR(S)
Nickolai Kukhtarev, Tatiana Kukhtareva and Sonia C. Gallegos

5d. PROJECT NUMBER
NNH00AL971

5e. TASK NUMBER

5f. WORK UNIT NUMBER
73-4214-09-5

7. PERFORMING ORGANIZATION NAME(S) AND ADDRESS(ES)
Naval Research Laboratory
Oceanography Division
Stennis Space Center, MS 39529-5004

8. PERFORMING ORGANIZATION REPORT NUMBER
NRL/JA/7330--10-0436

9. SPONSORING/MONITORING AGENCY NAME(S) AND ADDRESS(ES)
NASA Headquarters
Attn: Laurie Friederich
Mail Code 210.H, Bldg. 17, Rm. N111
Greenbelt, MD

10. SPONSOR/MONITOR'S ACRONYM(S)
NASA

11. SPONSOR/MONITOR'S REPORT NUMBER(S)

12. DISTRIBUTION/AVAILABILITY STATEMENT
Approved for public release, distribution is unlimited.

13. SUPPLEMENTARY NOTES

14. ABSTRACT

Application of single-beam reflective laser optical interferometry for oil films and droplets in water detection and characterization is discussed. Oil films can be detected by the appearance of characteristic interference patterns. Analytical expressions describing intensity distribution in these interference patterns allow determination of oil film thickness, size of oil droplets, and distance to the oil film from the observation plane. Results from these analyses indicate that oil spill aging and breakup can be monitored in real time by analyzing time-dependent holographic fringe patterns. Interferometric methods of oil spill detection and characterization can be automated using digital holography with three-dimensional reconstruction of the time-changing oil spill topography. In this effort, the interferometric methods were applied to samples from Chevron oil and British Petroleum MC252 oil obtained during the Deep Water Horizon oil spill in the Gulf of Mexico.

15. SUBJECT TERMS
holographic interferometry, oil-on-water film, coherent backscattering

16. SECURITY CLASSIFICATION OF:			17. LIMITATION OF ABSTRACT	18. NUMBER OF PAGES	19a. NAME OF RESPONSIBLE PERSON
a. REPORT	b. ABSTRACT	c. THIS PAGE			Sonia Gallegos
Unclassified	Unclassified	Unclassified	UL	5	19b. TELEPHONE NUMBER *(Include area code)* (228) 688-4867

Holographic interferometry of oil films and droplets in water with a single-beam mirror-type scheme

Nickolai Kukhtarev,[1,*] Tatiana Kukhtareva,[1] and Sonia C. Gallegos[2]

[1]Physics Department, Alabama A&M University, Normal, Alabama 35762, USA

[2]Naval Research Laboratory, Oceanography Division, Stennis Space Center, Mississippi 39529, USA

*Corresponding author: nickoly.kukhtarev@aamu.edu

Received 2 August 2010; revised 3 November 2010; accepted 6 November 2010; posted 9 November 2010 (Doc. ID 132657); published 7 January 2011

Application of single-beam reflective laser optical interferometry for oil films and droplets in water detection and characterization is discussed. Oil films can be detected by the appearance of characteristic interference patterns. Analytical expressions describing intensity distribution in these interference patterns allow determination of oil film thickness, size of oil droplets, and distance to the oil film from the observation plane. Results from these analyses indicate that oil spill aging and breakup can be monitored in real time by analyzing time-dependent holographic fringe patterns. Interferometric methods of oil spill detection and characterization can be automated using digital holography with three-dimensional reconstruction of the time-changing oil spill topography. In this effort, the interferometric methods were applied to samples from Chevron oil and British Petroleum MC252 oil obtained during the Deep Water Horizon oil spill in the Gulf of Mexico.

OCIS codes: 090.0090, 090.2880, 090.5694.

1. Introduction

Optical interferometry is a practical and popular method of detection and characterization of oil films and emulsified liquids. In this paper, we consider reflection geometry and briefly discuss different methods of optical interferometry with a focus on the detection and quantification of the thickness of oil spills on the water. Theoretical solution of the Maxwell wave equations [1] for reflection of electromagnetic waves from the oil films and droplets requires proper boundary and initial conditions. Backscattering from emulsified liquids was investigated in [2], and coherent backscattering measurement was applied for the study of microstructures in emulsified liquids. An enhanced component toward the backscattering direction emerges superimposed on the diffuse light scattering from a sample with randomly dispersed scatterers, giving evidence of the weak localization of light in random systems. Accurate measurement of the coherent backscattering peak gives us information on the optical transport mean free path in the sample, which leads to an estimation of the droplet size in emulsion. A new measurement system was developed and clear backscattering peaks were successfully observed for various kinds of emulsions. The key technique of the current experiment was to decrease the laser speckle by stirring the liquid. The result obtained for heptane/AOT [sodium bis(2-ethylhexyl)]/water emulsion was qualitatively related to the droplet size, which could be controlled by changing the amount of added salt. The effect of excluded volume on the scattering mean free path was discussed.

The reflectance of oil emulsion grows when wavelength increases with decreasing size of oil droplets in emulsion [3]. Another possibility for oil-film thickness determination is white-light interferometry [4,5], but it needs a more complex algorithm for deciphering the interference patterns in comparison with laser monochromatic interferometry.

The laser photophoretic behavior of an oil droplet in water emulsions was examined by radiating a

0003-6935/11/070B53-05$15.00/0

single-mode Nd:YAG laser (1064 nm) [6]. In the [6] emulsion systems examined, the photophoretic velocity ($\mu m\,s^{-1}$) of an organic droplet was found to be linearly proportional to both the laser power and the radius of the droplet. Furthermore, for droplets of the same size, the photophoretic mobility ($\mu m\,s^{-1}\,W^{-1}$), which means the photophoretic velocity normalized with the laser power, increased as the refractive index of the droplet increased. The dependence of the photophoretic mobility was discussed on the basis of a simple radiation theory in which the scattering force of a laser beam on a spherical droplet was formulated.

In this paper, we utilize samples from Chevron oil and British Petroleum (BP) light crude MC252 oil. We consider laser single-wavelength and single-beam interferometry as the most simple and reliable method of oil-film slick detection and quantification of the oil-film thickness and oil droplets. Reflected beams from the oil films and droplets on the water are described by a holographic approach as the interference of the signal wave reflected from the top of the oil spot with the reference beam reflected from the oil–water interface (for films) or from the water surface (for droplets and islands).

2. Experimental Setup and Modeling

A. Experimental Results

A simple scheme of holographic interferometry is shown in Fig. 1. A beam from an He–Ne laser (wavelength 0.632 μm), expanded by a lens ($F = 5$ cm), illuminates a sample of oil-on-water film at the near-vertical direction. The diameter of illuminated area at the sample is about 3 cm. Optical beams reflected from the top and bottom surfaces of the oil film form interference patterns on the screen (which was placed at a 6 m distance from the oil film). This interference pattern may be captured by the CCD camera and digitally processed. Examples of typical interferogram are shown in Fig. 2; photos were taken from the white diffusion screen. Because of differences in reflectance, thick oil film is seen as bright spots, while water appears as dark spots in the picture. The geometry of fringes reflects the thickness gradient of oil film and contains information about the oil-film topography. To recover topography information from the interference pattern, proper modeling of fringe pattern formation is needed.

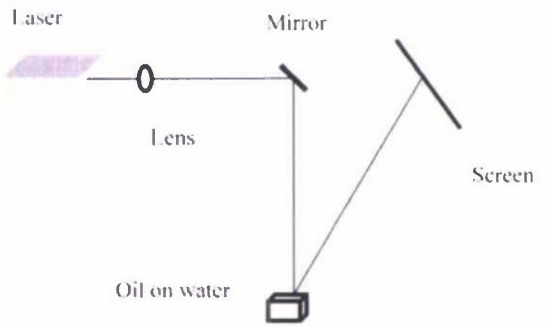

Fig. 1. Scheme of oil-on-water film interferometry; distance between oil film and screen ~6 m.

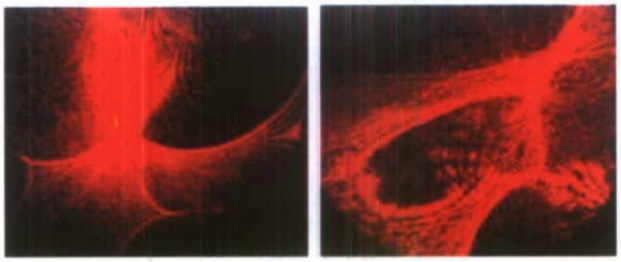

Fig. 2. (Color online) Typical interference patterns on reflection from the oil-on-water film under near-normal illumination by laser.

B. Modeling of Reflection from the Oil-on-Water Film

To find the reflection coefficient of the light wave with amplitude Eo from the oil-on-water film, we will consider a three-layer system (Fig. 3) air—1, oil film —2, and water—3, with refractive indices n_1, n_2, and n_3. The total reflected wave amplitude Er will be represented as a sum of the reflected wave from the front surface Ef and from the back surface Eb:

$$Er = Ef + Eb = (r_{12}E_0 + t_{12}t_{21}r_{23}E_0e^{i\Phi})e^{ikl}. \quad (1)$$

Here r_{12} and r_{23} are reflection coefficients from air–oil and oil–water, respectively, t_{12} and t_{21} are transmission coefficients from air–oil and from oil–air, k is the wavenumber $k = 2\pi/\lambda$, l is the distance along the propagation direction, and Φ is the phase shift between these two wave due to the optical path difference:

$$\Phi = 2kh[n_2^2 - (n_1 \sin\Theta)^2]^{1/2}. \quad (2)$$

In derivation of Eq. (2), we ignore multiple reflections, which is justified for the small reflection coefficients of the oil–water interface. For the slanted geometry of observations (not strictly vertical illumination), amplitude transmission/reflection coefficients depend on polarization that may be used for improvement of detection sensitivity.

For s-polarization [horizontal, perpendicular to the plane of incidence, or transverse electric (TE)], the coefficients for the air–water interface are [1]

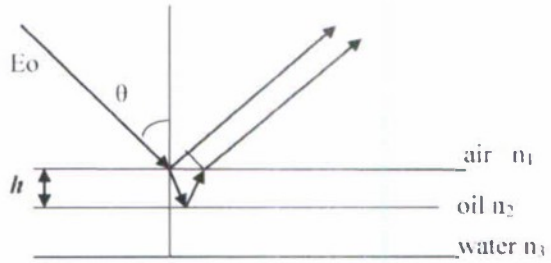

Fig. 3. Scheme of reflection of the wave with amplitude Eo from the oil film of thickness h with refractive index n_2 (refractive indices of air and water are n_1 and n_3, respectively).

$$r_{12} = \frac{n_1 \cos\vartheta - n_2 \cos\vartheta_t}{n_1 \cos\vartheta + n_2 \cos\vartheta_t},$$
$$t_{12} = 1 + r_{12} = \frac{2n_1 \cos\vartheta}{n_1 \cos\vartheta + n_2 \cos\vartheta_t}. \quad (3)$$

Here ϑ_t is the transmission angle, which is related to the incidence angle by

$$\cos\vartheta_t = \sqrt{1 - \left(\frac{n_1 \sin\vartheta}{n_2}\right)^2}.$$

It follows from Eq. (3) that, for $n_2 > n_1$ (as in our case of the air–water interface), the reflection coefficient is negative, which is the equivalent of a π-phase shift during reflection of s-polarized light.

For p-polarization [vertical, parallel to the plane of incidence, transverse magnetic (TM)], the coefficients will take the form

$$r_{12} = \frac{n_1 \cos\vartheta_t - n_2 \cos\vartheta}{n_1 \cos\vartheta_t + n_2 \cos\vartheta}. \quad (4)$$

For the transmission coefficient, we can get the expression

$$t_{12} = (1 + r_{12}) \frac{\cos\vartheta}{\cos\vartheta_t}. \quad (5)$$

For this TM polarization, there exists a Brewster angle of no reflection, defined by equating the reflection coefficient in Eq. (3) to zero.

The general approach for analysis of interference patterns is to find the first phase shift Φ using the expressions [7,8]

$$\Phi = \tan^{-1}\left(\frac{H(I)}{I}\right) \quad \text{where}$$
$$H(I(x)) = F^{-1}\left[F\left(\frac{1}{\pi x}\right) F(I(x))\right], \quad (6)$$

and $H(I(x))$ is the Hilbert transform of the intensity signal, F represents the Fourier transform, and F^{-1} is the inverse Fourier transform. Once the phase has been determined, the oil-film height can be found from Eq. (2). As it was mentioned in [9], comparison of TE and TM polarizations for the film interferometry show that TM polarization gives better visibility and so is more sensitive for oil-film characterization.

C. Reflection from the Oil Droplets

For those types of oil whose refractive indices are not very different from that of water, thin-film interference will give low-contrast patterns that are difficult to analyze. In such cases, interference patterns arising from the reflection from oil droplets and islands will be more pronounced. Modeling of interference patterns in this case can be done in a way that is similar to wavefront division interferometry with a reference wave created by reflection of the plane wave from the water surface. The signal wave will be produced by reflection of part of the laser wave from the curved surface of the oil droplet. Interference of these copropagating waves produces interference patterns that depend on the oil droplet thickness.

Scattering of light by spherical particles has been intensively studied by Mie theory [10,11] and later was extended to nonspherical particles [11,12]. The special case of the forward scattering in the far zone may be also described as single-beam (or in-line) holography.

From Mie theory [10], the backward scattered electric field is given by

$$E_s = e^{-ikr - ikz} S E_0/(ikr). \quad (7)$$

Here, k is the wave number, S is the scattering amplitude, and E_0 is the incident plain wave. In the point x, y, z in the backward direction, since $x, y \ll z$ we have

$$r = \sqrt{x^2 + y^2 + z^2} \approx z + \frac{x^2 + y^2}{2z}. \quad (8)$$

Superposition of the incident (reference) and scattered (signal) waves give total amplitude

$$E = E_s + E_0 = E_0[1 + e^{-ik(x^2+y^2)/2z} S/(ikz)]. \quad (9)$$

For intensity I in approximation of $E_s \ll E_0$, we will get

$$I = [E]^2 = I_0\left(1 + \frac{2}{kz}\mathrm{Re}[-iSe^{-ik(x^2+y^2)/2z}]\right), \quad (10)$$

where Re = real part.

For radius of the scattering particle $a \gg$ (laser wavelength), the scattering amplitude is, for perpendicular polarization [13,14],

$$S(\vartheta) = \beta^2\left(J_1(\gamma)/\gamma + \frac{i\rho'\xi(\delta)}{\delta^2} + \frac{J_0(\gamma)}{\rho^2}\right),$$
$$\xi(\delta) = \frac{\sin\delta}{\delta} - \cos\delta + i\left[\frac{\cos\delta}{\delta} - \sin\delta\right],$$
$$\delta = \sqrt{\gamma^2 + \rho^2}, \qquad \beta = \frac{2\pi}{\lambda}a,$$
$$\gamma = 2\beta\sin\vartheta/2, \qquad \rho = 2(n-1)\beta,$$
$$\rho' = 2(n'-1)\beta, \quad (11)$$

where n is the refractive index of spherical particles (oil droplet) $n = n' - in''$, J_1 and J_0 are the Bessel functions of the first and zero orders, θ is the polar angle and a is the radius of curvature for the spherical particle.

The first term in Eq. (11) is the diffracted term. The second term includes the refracted light term (in

geometric optics approximation) and depends on the refractive index. The last term is more pronounced for smaller particles and is due to interaction between the refracted and diffracted components.

From the analysis of the extrema of the interference pattern [10], the radius of the particle a and the distance of the particle to the screen z can be found.

For illustration, we will consider analysis of the interference pattern when only the first, diffraction term is important.

To find the size of the diffracting droplet, we need to equal the Bessel argument kar_1/z to the values that reduce it to zero (here $r_1 = (x^2 + y^2)^{1/2}$).

As an example of both radial and density plots, extrema (Fig. 4) of sin (at ~0.16 cm) and Bessel functions (at ~ 0.6 cm) are easily noticeable, which allows us to find distance $z = 800$ cm and droplet size $a = 0.5$ mm.

3. Kinetics of Oil-Film Aging and Dispersion by Corexit 9500

Application of dispersant Corexit 9500 to the oil samples allows monitoring of the oil breakup and aging [15]. Figure 5 depicts a sequence of photos that shows

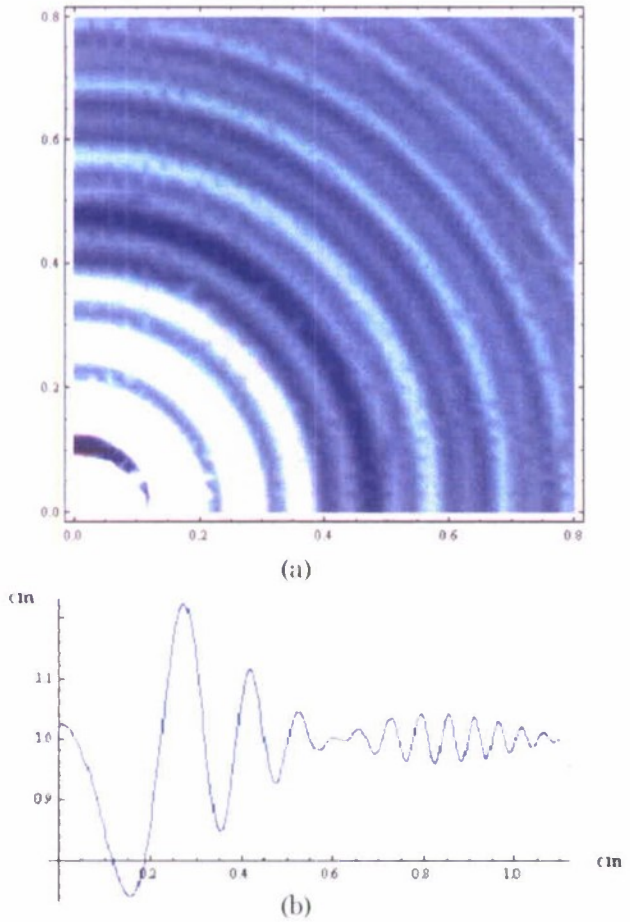

Fig. 4. (Color online) (a) Density plot and (b) radial dependence of the hologram intensity for parameters $a = 0.5$ mm, $z = 800$ cm, wavelength 0.633 μm).

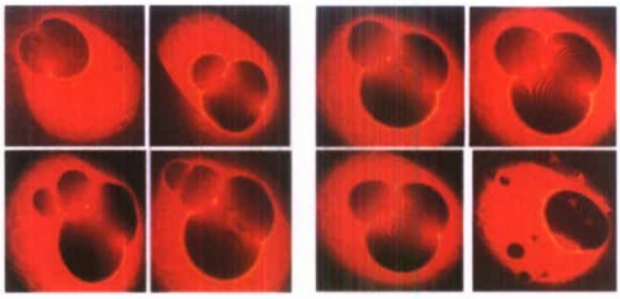

Fig. 5. (Color online) Kinetics of oil-film aging after applying dispersant Corexit 9500 (top left to bottom right); photos were taken at 3 s intervals (diameter of the illuminated oil-film area was about 3 cm). The last (bottom) picture shows breakup of a big oil island with the formation of droplets.

the kinetics of the oil spot thinning and breaking up upon application of the liquid dispersant to the film. All photos were taken from the images projected on the white diffusion-scattering screen. Figure 5 shows that only the relatively smooth part of the kinetic, initial stage of oil dispersion was much faster (about 1 s) and was followed by the abrupt spatial separation of fragments. After this (fast) initial stage, smoother changes with relatively small separation were captured by the interference method, as shown in Fig. 5.

For observation of the initial (fast) stage of the oil-film dispersion, modification of the interferometric experiment is needed, including illumination with a larger-diameter laser spot to allow capture of the diverging oil-film fragments.

4. Discussion and Conclusion

We have discussed application of single-beam laser optical interferometry for detection and characterization of oil films, islands, and droplets on water. Detection of oil films can be done by observation of characteristic interference patterns. Analytical expressions describing intensity distribution in these interference patterns allows finding the thickness of the oil films, the size of oil droplets, and the distance to the oil film from the observation plane.

Estimates of the oil-film thickness can be accomplished by counting fringes on the interferogram [Fig. 2(b)] at the edge of the oil spot. By multiplying the number of fringes (about six) on the laser wavelength (0.633 μm), we get a film thickness value of 3.8 μm. By modeling of the interferogram of a droplet, we show that both droplet size and its distance to the observation plane can be found from the analysis of the interferogram fringes. In addition, it is possible to observe the kinetics of oil slick aging by monitoring the time dependence of fringes. Interferometric methods of oil spill detection and characterization can be automated by using a decision-making digital approach with proper programming [9] that includes three-dimensional reconstruction of the oil topography.

This work was supported by the Title III Program of the Alabama A&M University for T. Kukhtareva and an American Society for Engineering Education/Office of Naval Research (ONR) Summer Fellowship for N. Kukhtarev. Support for S. C. Gallegos was provided by NASA-ROSES 2008 NNH08ZDA001N: A28: Earth Science for Decision Making: Gulf of Mexico Region. Special thanks are extended to Chevron Pascagoula refinery for providing crude oil samples and to M. Ben Kinney from Exponent, Inc. for supplying the dispersant samples utilized in this study.

References

1. D. K. Cheng, *Fundamentals of Engineering Electromagnetics* (Addison-Wesley, 1994).
2. S. Mitani, K. Sakai, and K. Takagi, "Measurement of coherent backscattering phenomena in emulsion" Jpn. J. Appl. Phys. **38**, 1398–1402 (1999).
3. Z. Otremba, "Oil-in-water emulsion as a modifier of water reflectance," Opt. Appl. **39**, 123–128 (2009).
4. E. Ciulli, T. Draexl, and K. Stadler, "Film thickness analysis for EHL contacts under steady-state conditions by automatic digital image processing," Adv. Tribology **2008**, 325187 (2008).
5. C. Sun, L. Yu, Y. Sun, and Q. Yu, "Scanning white-light interferometer for measurement of the thickness of a transparent oil film on water," Appl. Opt. **44**, 5202–5205, (2005).
6. A. Hirai, H. Monjushiro, and H. Watarai, "Laser photophoresis of a single droplet in oil in water emulsions," Langmuir **12**, 5570–5575 (1996).
7. J. W. Naughton and M. Sheplak, "Modern developments in shear-stress measurement," Prog. Aerosp. Sci. **38**, 515–570 (2002).
8. P. Merati, E. Van Meter, and J. Schmitz, "Shear stress measurement by the thin oil film technique," Technical Report MAE-04-05 (Western Michigan University, 2004).
9. Y.-C. Huang and U. C. Liang, "Interferometric oil-spill detection system," Opt. Eng. **40**, 740–746 (2001).
10. K.-N. Liou, "A complimentary theory of light scattering by homogeneous spheres," Appl. Math. Comput. **3**, 331–358 (1977).
11. O. N. Ross and S. G. Bradley, "Model for optical scattering by nonspherical raindrops," Appl. Opt. **41**, 5130–5141 (2002).
12. Ju. A. Eremin, N. V. Orlov, and V. I. Rosenberg, "Electromagnetic scattering from single electrified raindrops," J. Atmos. Terr. Phys. **57**, 141–149 (1995).
13. N. M. Nussenzveig, "Complex angular momentum theory of rainbow and the glory," J. Opt. Soc. Am. **69**, 1068–1079 (1979).
14. M. Jonasz and G. Fournier, *Light Scattering by Particles in Water, Theoretical and Experimental Foundations* (Elsevier, 2007).
15. B. Gopalan and J. Katz, "Turbulent shearing of crude oil mixed with dispersants generates long microthreads and microdroplets," Phys. Rev. Lett. **104**, 054501 (2010).